Identification of elastic and damping properties of sandwich structures based on high resolution modal analysis of point measurements

Marc Rébillat, Xavier Boutillon

Identification of elastic and damping properties of sandwich structures based on high resolution modal analysis of point measurements.

M. Rébillat [1,2], **X. Boutillon** [1]
[1] LMS-CNRS, École Polytechnique, 91128 Palaiseau Cedex, France
e-mail: **rebillat@lms.polytechnique.fr**

[2] LIMSI-CNRS, Université Paris-Sud, B.P. 133, 91403 Orsay Cedex, France.

Abstract

A method is proposed to identify the mechanical properties of the skin and core materials of sandwich structures having heterogeneous cores. All the elastic coefficients and loss-factors that matter in the dynamics of such a panel in the thick-plate approximation are identified. To this end, experimental natural modes (i.e. eigenmodes of the damped system) are compared to the numerical modes of large sandwich panels ($l_{x,y}/h \simeq 80$). The chosen generic model for the visco-elastic behaviour of the materials is $E(1 + j\eta)$. The numerical modes are computed by means of a Rayleigh-Ritz procedure and their dampings are predicted according to the visco-elastic model. The frequencies and dampings of the natural modes of the panel are estimated experimentally by means of a high-resolution modal analysis technique. An optimisation procedure yields the desired coefficients. A sensitivity analysis assess the reliability of the method. Identification is conducted on two very different kind of sandwich panels to illustrate the method.

1 Introduction

Because of their light weight and the easy adjustment of their mechanical properties, sandwich structures with an heterogeneous core are widely used nowadays. However, due to the heterogeneities, their structural mechanical properties are difficult to predict accurately on the basis of the material properties and identification procedures are often needed. Mixed numerical (Num) / experimental (XP) methods are used to identify the parameters of a model by comparing simulated and measured characteristics (for example modal dampings α_n^{Num} vs. α_n^{XP} and frequencies f_n^{Num} vs. f_n^{XP} of the first modes of the system). In order to obtain good identification results, the model parameters must be sensitive to the measured characteristics.

Several authors have addressed the problem of the identification of elastic and damping properties of homogeneous thick plates from full field measurements [1, 2, 3] or of homogeneous thin plates using point measurements [4, 5, 6]. However no method has yet been presented for the identification of elastic and damping properties of thick plates from point measurements.

Sandwich panels often raise special difficulties because of their heterogeneous cores (honeycombs core for example). Equivalent elastic properties of such sandwich plates can be identified [7, 8], but obtaining their damping properties is still challenging. Following the work of De Visscher *et al.* [4] a point measurement method for the identification of the elastic and damping properties of sandwich panels with heterogeneous cores is presented in this paper, based on a thick plate approximation.

In order to consider the sandwich core as homogeneous in the in-plane directions, up to a given frequency f, the corresponding wavelength λ must contain at least 50 cells [9]. For a typical cell side-length s_{cell} and height h this implies that the dimensions of a panel must be such that $l_{x,y} > \lambda > 50\, s_{cell}$. On the other hand, the panel must appear as a thick-plate (rather than a thin-plate) if the *out-of-plane* elastic and damping properties are to be identified. For flexural waves this implies that high-enough frequencies are included in the processed data: $\lambda/h \leq 6$ [10]. In other words, the panel must be large enough and the observed dynamics must include high-enough modes, within the limit of a plate model. Due to the intrinsic dissipations of the materials, the modal characteristics of high modes may be difficult to measure with the Fourier transform (FT) which is limited to modal overlaps of $\simeq$ 30 % in most implementations. The high-resolution modal analysis (HRMA) technique [11] is an alternative to the FT for the estimation of modal parameters up to a modal overlap of $\simeq$ 70 %.

In the present work, the identification of most elastic and damping properties of sandwich structures with an heterogeneous core is considered by means of the modal analysis of large panels ($l_{x,y}/h \simeq 80$). The HRMA technique is used to estimate modal frequencies and dampings of the first $\simeq$ 40 modes of the panels. An optimisation procedure, based on a numerical thick-plate model is used afterwards to identify the corresponding elastic and damping properties.

2 A mechanical model of sandwich panels

2.1 Hypotheses

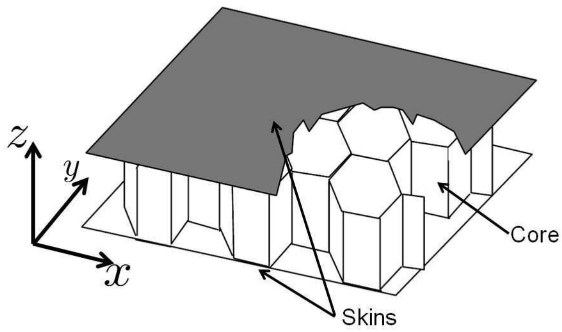

Figure 1: Geometry of the sandwich plate.

The sandwich panel consists in two identical skins and a core (Fig. 1). The thicknesses of the core and the skins are h^c and h^s respectively. The thickness of the panel is $h = h^c + 2h^s$. In the following, ”panel” designs the physical structure whereas ”plate” refers to the idealized structure made out of the equivalent homogeneous material. The following hypotheses are made on the panel and plate:

- Displacements are small so that the materials and structures behave linearly.
- Only flexural waves are considered.
- The plate is considered to follow the Reissner-Mindlin approximations (thick-plate model). For the aspect ratio $l_{x,y}/h > 80$ of the panels under study, a more sophisticated theory such as “Third Order Shear Deformation Theory” would not give significantly different modal frequencies and dampings [12].
- The wavelengths include at least 50 cells. According to Burton *et al.* [9], this ensures that errors on the modal frequencies of the plate (with a homogeneous equivalent core) are less than 2% when compared to those of the panel as computed by various FE-models.

The skin and core materials are each considered as homogeneous, orthotropic in the x and y directions, and viscoelastic.

The formalism chosen for describing the viscoelastic behaviour is that of complex moduli $\underline{E} = E(1 + j\eta)$ which do not depend on the frequency (see the model of materials in section 2.2). The Young's and shear moduli and the Poisson coefficient of the core are $\underline{E}_x^c$, $\underline{E}_y^c$, $\underline{E}_z^c$, $\underline{G}_{xy}^c$, $\underline{G}_{xz}^c$, $\underline{G}_{yz}^c$, $\underline{\nu}_{yx}^c$, $\underline{\nu}_{xz}^c$, $\underline{\nu}_{yz}^c$ and $\underline{\nu}_{xy}^c$. The same parameters for the skins are denoted by the s index. The properties of the homogeneous material equivalent to the whole sandwich are denoted by the H index.

The following hypotheses are made on the sandwich panel:

- The sandwich panel is symmetric with respect to its mid-plane.
- Skins are very thin compared to the core so that shear stress in the skin can be ignored: $h^s G_{xz}^s \ll h^c G_{xz}^c$ (and the same in the y direction).
- The core is considered to be very soft ($E_x^c \ll E_x^s$, $E_y^c \ll E_y^s$ and $G_{xy}^c \ll G_{xy}^s$). Given the generic expression of the moduli of the homogeneous equivalent material $E^H = \left(\frac{h^c}{h}\right)^3 E^c + \left[1 - \left(\frac{h^c}{h}\right)^3\right] E^s$, this ensures that all in-plane stress in the plate are entirely due to those in the skins.

According to these hypotheses, there is no stress associated with $\underline{E}_z^{c,s,H}$, $\underline{\nu}_{xz}^{c,s,H}$, $\underline{\nu}_{yz}^{c,s,H}$, $\underline{G}_{xz}^s$, $\underline{G}_{yz}^s$, $\underline{E}_x^c$, $\underline{E}_y^c$, $\underline{G}_{xy}^c$, $\underline{\nu}_{xy}^c$, $\underline{\nu}_{yx}^c$ which are ignored in what follows. These hypotheses are generally fulfilled in common sandwich panels. The typical orders of magnitude for the considered parameters in this kind of sandwich panels are:

$$\begin{cases} h^s/h^c \simeq 10^{-1} \\ E_x^c/E_x^s \simeq E_y^c/E_y^s \simeq G_{xy}^c/G_{xy}^s \simeq 10^{-5} \end{cases} \tag{1}$$

2.2 Model of the materials

The damping of plate vibrations has different origins. In the present study, it is assumed that panels vibrate below their coincidence acoustical frequencies. Consequently, damping due to acoustical radiation in surrounding air is very small compared to the structural damping. Among the different structural damping models, we have retained the standard hysteretic model (which is frequency-independent, see for example [13]). The relationship between the stress $\boldsymbol{\epsilon}^\gamma$ and the strain $\boldsymbol{\sigma}^\gamma$ in each $\gamma-$material ($\gamma = s, c$, or H) involves 7 complex numbers and can be written, to first order in η as:

$$\boldsymbol{\sigma}^\gamma = \begin{bmatrix} E_x^\gamma(1 + j\eta_x^\gamma) & \nu_{yx}^\gamma E_x^\gamma[1 + j(\eta_{\nu_{yx}}^\gamma + \eta_x^\gamma)] & 0 & 0 & 0 \\ \nu_{xy}^\gamma E_y^\gamma[1 + j(\eta_{\nu_{xy}}^\gamma + \eta_y^\gamma)] & E_y^\gamma(1 + j\eta_y^\gamma) & 0 & 0 & 0 \\ 0 & 0 & G_{xz}^\gamma(1 + j\eta_{xz}^\gamma) & 0 & 0 \\ 0 & 0 & 0 & G_{yz}^\gamma(1 + j\eta_{yz}^\gamma) & 0 \\ 0 & 0 & 0 & 0 & G_{xy}^\gamma(1 + j\eta_{xy}^\gamma) \end{bmatrix} \boldsymbol{\epsilon}^\gamma \tag{2}$$

The symmetry of the strain/stress relation adds the following relationships $\nu_{xy}^\gamma E_y^\gamma = \nu_{yx}^\gamma E_x^\gamma$ and $\eta_{\nu_{xy}}^\gamma + \eta_y^\gamma = \eta_{\nu_{yx}}^\gamma + \eta_x^\gamma$ which leaves 12 independent real parameters to be identified for each material (24 altogether). In order to keep a formal symmetry in the mathematical treatment, one defines[1]:

$$\nu^\gamma = \sqrt{\nu_{xy}^\gamma \nu_{yx}^\gamma} \qquad \eta_\nu^\gamma = \eta_{\nu_{xy}}^\gamma + \eta_y^\gamma \tag{3}$$

[1]One must keep in mind that η_ν^γ is *not* the imaginary part of $\underline{\nu}^\gamma$.

2.3 Equivalent thick plate

Under the hypothesis and for the orders of magnitude given in section 2.1, the sandwich panel behaves in the low frequency range like a homogeneous thick-plate [14]. The thickness of the plate is chosen to be h. Its mechanical properties are given in Eq. (4) and (5) as functions of the mechanical and geometrical properties of the skins and the core.

$$\begin{cases} E_x^H = E_x^s\left[1-\left(\dfrac{h^c}{h}\right)^3\right] \quad E_y^H = E_y^s\left[1-\left(\dfrac{h^c}{h}\right)^3\right] \quad \nu^H = \nu^s \\ G_{xy}^H = G_{xy}^s\left[1-\left(\dfrac{h^c}{h}\right)^3\right] \quad G_{xz}^H = G_{xz}^c \quad G_{yz}^H = G_{yz}^c \end{cases} \tag{4}$$

$$\begin{cases} \eta_x^H = \eta_x^c \dfrac{E_x^c}{E_x^s}\left(\dfrac{h^c}{h}\right)^3 + \eta_x^s\left[1-\left(\dfrac{h^c}{h}\right)^3\right] \quad \eta_y^H = \eta_y^c \dfrac{E_y^c}{E_y^s}\left(\dfrac{h^c}{h}\right)^3 + \eta_y^s\left[1-\left(\dfrac{h^c}{h}\right)^3\right] \\ \eta_{xy}^H = \eta_{xy}^c \dfrac{G_{xy}^c}{G_{xy}^s}\left(\dfrac{h^c}{h}\right)^3 + \eta_{xy}^s\left[1-\left(\dfrac{h^c}{h}\right)^3\right] \quad \eta_{xz}^H = \eta_{xz}^c \quad \eta_{yz}^H = \eta_{yz}^c \quad \eta_\nu^H = \eta_\nu^s \end{cases} \tag{5}$$

The 12 independent real parameters $\{E_x^H, \eta_x^H, E_y^H, \eta_y^H, G_{xy}^H, \eta_{xy}^H, G_{xz}^H, \eta_{xz}^H, G_{yz}^H, \eta_{yz}^H, \nu^H, \eta_\nu^H\}$ are to be identified. Their knowledge yields the elastic and damping properties of each layer of the sandwich panel provided that the 12-equation system formed by Eqs. (4) and (5) is invertible. A sufficient condition is:

$$\eta_x^c \frac{E_x^c}{E_x^s} \ll \eta_x^s \quad \eta_y^c \frac{E_y^c}{E_y^s} \ll \eta_y^s \quad \eta_{xy}^c \frac{G_{xy}^c}{G_{xy}^s} \ll \eta_{xy}^s \tag{6}$$

since $\dfrac{E_x^c}{E_x^s} \ll 1$, $\dfrac{E_y^c}{E_y^s} \ll 1$, and $\dfrac{G_{xy}^c}{G_{xy}^s} \ll 1$ (see last point in section 2.1). This condition is not satisfied only if the η^c-coefficients are several orders of magnitude larger than the η^s-ones. This is not the case here and rarely the case in general[2]. Consequently, the identification of the E_x^H, *etc* ... yields a measurement of the mechanical properties of the skin and core materials.

2.4 Potential, kinetic and dissipated energies in the equivalent thick-plate

Within the frame of the first order Reissner-Mindlin theory the displacements $\{u, v, w\}$ in the $\{x, y, z\}$-directions respectively are [15]:

$$u(x,y,z,t) = -z\Phi_x(x,y,t) \qquad v(x,y,z,t) = -z\Phi_y(x,y,t) \qquad w(x,y,z,t) = w_0(x,y,t) \tag{7}$$

The potential energy of the plate is:

$$\begin{aligned} U &= \frac{1}{2}\iiint_{\mathcal{V}} (\boldsymbol{\sigma}^H)^T \boldsymbol{\epsilon}^H \, \mathrm{d}\tau \\ &= \frac{1}{2}\iint_S \Bigg[D_1\left(\frac{\partial \Phi_x}{\partial x}\right)^2 + D_2\left(\frac{\partial \Phi_x}{\partial x}\frac{\partial \Phi_y}{\partial y}\right) + D_3\left(\frac{\partial \Phi_y}{\partial y}\right)^2 + D_4\left(\Phi_y^2 - 2\Phi_y\frac{\partial w_0}{\partial y} + \left(\frac{\partial w_0}{\partial y}\right)^2\right) + ... \\ &\qquad D_5\left(\Phi_x^2 - 2\Phi_x\frac{\partial w_0}{\partial x} + \left(\frac{\partial w_0}{\partial x}\right)^2\right) + D_6\left(\left(\frac{\partial \Phi_x}{\partial y}\right)^2 + 2\frac{\partial \Phi_x}{\partial y}\frac{\partial \Phi_y}{\partial x} + \left(\frac{\partial \Phi_y}{\partial x}\right)^2\right)\Bigg]\mathrm{d}x\mathrm{d}y \end{aligned} \tag{8}$$

[2]It can be the case when skins are made of metal and the core is made of paper honeycombs or of viscoelastic foam.

with

$$D_1 = \frac{E_x^H h^3}{12(1-\nu_{xy}\nu_{yx})} \qquad D_2 = \frac{\nu_{xy}E_y^H h^3}{6(1-\nu_{xy}\nu_{yx})} \qquad D_3 = \frac{E_y^H h^3}{12(1-\nu_{xy}\nu_{yx})}$$
$$D_4 = 2\kappa_{yz}^2 h G_{yz} \qquad D_5 = 2\kappa_{xz}^2 h G_{xz} \qquad D_6 = \frac{G_{yz}h^3}{6} \tag{9}$$

The shear correction factors κ_{yz}^2 and κ_{xz}^2 account for the fact that Eq. (7) is an approximation: the $\Phi_{x,y}$ coefficients depend lightly on z and sections of the plate do not remain plane in the flexural deformation. The values $\kappa_{yz} = \kappa_{xz} = 1$ have been chosen according to the recommendations of [16] for sandwich panels.

By definition, the fraction of energy lost during one cycle is:

$$\Delta U \quad = - \int_{\mathcal{T}} \left[\quad \iiint_{\mathcal{V}} (\boldsymbol{\sigma}^H)^T \frac{\partial \boldsymbol{\epsilon}^H}{\partial t} \, \mathrm{d}\tau \right] \mathrm{d}t \tag{10}$$

Based on section 2.2, ΔU can then be expressed as:

$$\begin{aligned}\Delta U \quad = -\pi \quad \iint_{\mathcal{S}} \Bigg[& \eta_x^H D_1 \left(\frac{\partial \Phi_x}{\partial x}\right)^2 + \eta_\nu^H D_2 \left(\frac{\partial \Phi_x}{\partial x}\frac{\partial \Phi_y}{\partial y}\right) + \eta_y^H D_3 \left(\frac{\partial \Phi_y}{\partial y}\right)^2 + \eta_{yz}^H D_4 \left(\Phi_y^2 - 2\Phi_y \frac{\partial w_0}{\partial y} + \left(\frac{\partial w_0}{\partial y}\right)^2\right) + \dots \\ & \eta_{xz}^H D_5 \left(\Phi_x^2 - 2\Phi_x \frac{\partial w_0}{\partial x} + \left(\frac{\partial w_0}{\partial x}\right)^2\right) + \eta_{xy}^H D_6 \left(\left(\frac{\partial \Phi_x}{\partial y}\right)^2 + 2\frac{\partial \Phi_x}{\partial y}\frac{\partial \Phi_y}{\partial x} + \left(\frac{\partial \Phi_y}{\partial x}\right)^2\right)\Bigg] \mathrm{d}x\mathrm{d}y\end{aligned} \tag{11}$$

The kinetic energy T of the system is given in Eq. (12) as a function of Φ_x, Φ_y, and w_0. In this expression, ρ^H is the density of the equivalent homogeneous thick plate which is given by $h\rho^H = h^c\rho^c + 2h^s\rho^s$.

$$T = \frac{\rho^H \omega^2}{2} \iiint_{(\mathcal{V})} \left[u^2 + v^2 + w^2\right] \mathrm{d}\tau = \frac{\rho^H \omega^2}{2} \iint_{(\mathcal{S})} \left[\frac{h^3}{12}(\Phi_x^2 + \Phi_y^2) + h w_0^2\right] \mathrm{d}x\mathrm{d}y \tag{12}$$

3 Numerical model of the thick plate

In order to compare experimental results to numerical simulations, it is necessary to evaluate the damping factors of numerical modes. The dynamics of the panel is given by the hypotheses listed in section 2.1, the Eqs. (2), and the boundary conditions. Instead of a direct time-integration of the motion, we model here the damping of the numerical modes of the associated conservative system, under the hyptothesis of light damping. The problem consists in evaluating the relationships between the α_n^{Num} damping factors and the η^H loss-factors.

3.1 Modal representation

The honeycomb sandwich panel is considered here as a non conservative system $\mathcal{P}_{NC}$ with N degrees of freedom $\boldsymbol{q} = \{q_n\}$ where $\boldsymbol{q}$ is any set of generalised displacements. The damping model presented in section 2.2 corresponds to viscous damping. Under this hypothesis, the equation of the free motion of $\mathcal{P}_{NC}$ can be written as:

$$\boldsymbol{M}\ddot{\boldsymbol{q}} + \boldsymbol{C}\dot{\boldsymbol{q}} + \boldsymbol{K}\boldsymbol{q} = 0 \tag{13}$$

where $\boldsymbol{M}$, $\boldsymbol{C}$ and $\boldsymbol{K}$ are the mass, damping, and stiffness matrices. In what follows, the modes of $\mathcal{P}_{NC}$ are called natural modes. We also refer to the associated conservative system $\mathcal{P}_C$ corresponding to $\boldsymbol{C} = 0$. The modes of $\mathcal{P}_C$ will be noted $\boldsymbol{\xi}_n$ and associated with the normal frequencies f_n.

If $\mathcal{P}_{NC}$ is lightly damped, it can be shown [17] that the natural modes are $\boldsymbol{\xi}_n$ and the natural frequencies are $f_n + j\alpha_n$ to first order.

Let U_n^{NC} be the potential energy associated with the n^{th} mode of $\mathcal{P}_{NC}$. It varies in time as $\exp(-2\alpha_n t)$ so that the energy lost by this mode during one cycle ΔU_n^{NC} is:

$$\Delta U_n^{NC} = -2\frac{\alpha_n}{f_n} U_n^{NC} \tag{14}$$

Since $\mathcal{P}_C$ and $\mathcal{P}_{NC}$ have the same modes, $U_n^{NC} = U_n^C$. And since $U_n^C = T_n^C$, one obtains:

$$\Delta U_n^{NC} = -2\frac{\alpha_n}{f_n} T_n^C \tag{15}$$

Once the modes $\boldsymbol{\xi}_n$ of $\mathcal{P}_C$ (and of $\mathcal{P}_{NC}$) are known, Eqs. (8), (11), and (14) yield the modal dampings α_n of $\mathcal{P}_{NC}$.

3.2 Rayleigh-Ritz procedure for the conservative modes

A Rayleigh-Ritz procedure has been used to derive the mode shapes $\boldsymbol{\xi}_n^{Num}$ and the modal frequencies f_n^{Num} of $\mathcal{P}_C$. To this end, the generalised displacements $\Phi_x(x,y)$, $\Phi_y(x,y)$, and $w_0(x,y)$ have been projected on an orthonormal polynomial basis of order Q satisfying the free-free boundary conditions [18]:

$$\Phi_x(x,y) = \sum_{i,j} L_{ij} p_i(x) p_j(y) \quad \Phi_y(x,y) = \sum_{i,j} M_{ij} p_i(x) p_j(y) \quad w_0(x,y) = \sum_{i,j} N_{ij} p_i(x) p_j(y) \tag{16}$$

This procedure generates a new set of generalised displacements L_{ij}, M_{ij} and N_{ij}. The kinetic and potential energies T and U, defined in section 2.4, have been expressed explicitly as functions of the new coordinates. The Hamilton principle reads as:

$$\forall (i,j) \in [0, Q-1]^2 : \ \frac{\partial (T-U)}{\partial L_{ij}} = 0 \quad \frac{\partial (T-U)}{\partial M_{ij}} = 0 \quad \frac{\partial (T-U)}{\partial N_{ij}} = 0 \tag{17}$$

The above system of $3Q^2$ linear equations can be re-written as $[\boldsymbol{K} - 4\pi^2 f^2 \boldsymbol{M}]\boldsymbol{\xi} = 0$, see also Eq. (13), where f is the eigenfrequency and $\boldsymbol{\xi}$ is the eigenvector of unknown coefficients L_{ij}, M_{ij} and N_{ij}. The resolution of this eigenvalue problem gives a straightforward access to the modal frequencies f_n^{Num} and mode shapes $\boldsymbol{\xi}_n^{Num}$ of $\mathcal{P}_C$.

3.3 Derivation of α_n^{Num}

By introducing the numerical modes $\boldsymbol{\xi}_n^{Num}$ and frequencies f_n^{Num} found in section 3.2 in the energies expressions of section 2.4, the relations Eqs. (18) are obtained. The coefficients t_n and u_{nk} depend only on the geometry and mass parameters of the plate and on the modal shape $\boldsymbol{\xi}_n^{Num}$. For the subscripts of η, $\{x, v, y, yz, xz, xy\}$ have been replaced by $\{1, 2, 3, 4, 5, 6\}$.

$$\forall n \in [1, N] : \quad U_n^{NC} = U_n^C = \sum_{k=1}^{6} D_k u_{nk} \quad \Delta U_n^{NC} = -\pi \sum_{k=1}^{6} \eta_k D_k u_{nk} \quad T_n^C = 4\pi^2 f_n^2 t_n \tag{18}$$

Using relations Eqs. (18), the expression Eq. (19) of the modal dampings α_n^{Num} can be deduced from Eq. (15). One can notice than α_n is a linear combination of the η_k.

$$\alpha_n = \frac{f_n \Delta U_n^{NC}}{2T_n^C} = \sum_{k=1}^{6} \eta_k D_k \frac{u_{nk}}{4\pi f_n t_n} \tag{19}$$

4 Experimental study of sandwich panels

4.1 Experimental setup

Two different sandwich panels with heterogeneous cores have been studied experimentally. The first one is a rectangular lightweight honeycomb sandwich panel (Nomex® honeycombs core and paper skins). The second one is a sandwich sheet composed of two stainless steel face sheets and two bidirectionally corrugated steel layers form its core of 20 % relative density. Known parameters for each panels are given in Table 1. Since $l_{x,y}/h \simeq 80$ for the honeycombs core panel and $l_{x,y}/h \simeq 90$ for the bidirectionally corrugated core one, they both satisfy the Reissner-Mindlin approximations (see Sec. 2.1). Panels were suspended by thin wires in order to ensure free-free boundary conditions. The honeycomb core panel has been acoustically excited by an electro-dynamical loudspeaker placed in its vicinity and driven by a wide-band electrical signal. Its response was measured with a laser vibrometer pointing one corner. This ensures that all modes are present in the response. By means of a specially designed excitation signal [19], the impulse response of the panel was reconstructed. The corrugated core panel has been excited at different positions by means of an impact hammer. The panel responses were measured with an accelerometer located in one corner. Impulse responses were obtained after deconvolution with the force signal.

	l_x	l_y	h^s	h^c	s_{cell}	ρ^c	ρ^s
Honeycomb core panel	39.15 cm	59.10 cm	0.2 mm	4.88 mm	4 mm	37.8 kg/m^3	713 kg/m^3
Corrugated core panel	17.78 cm	22.86 cm	0.2 mm	1.48 mm	1 mm	2164 kg/m^3	7800 kg/m^3

Table 1: Geometry and mass of each sandwich panels. The typical length of the core-cells is denoted s_{cell}.

4.2 High resolution modal analysis

The impulse response of the non-conservative system can be expressed as a summation over its natural modes:

$$h(t) = \sum_{n=1}^{N} \xi_n \exp(j2\pi f_n t - \alpha_n t + j\phi_n) \tag{20}$$

In order to extract the experimental modal frequencies f_n^{XP} and dampings α_n^{XP}, a recently developed modal analysis method [11] has been applied to velocity impulse responses of the sandwich panels obtained in section 4.1. In the available noise conditions, the parameters of the 45 first modes could be extracted for the honeycombs core panel and of the 38 first modes for the corrugated core panel. The modal overlap of the highest modes of the honeycombs core sandwich panel was $\simeq$ 50 %, which is out of reach of traditional implementations of the Fourier transform, hence our need of the new method.

Using several bandpass filters associated with the ESPRIT and ESTER algorithms (see reference [11] for details), it is shown that this method yields a precise estimation of f_n and α_n in presence of moderate noise: the modal frequencies f_n can be estimated with a precision of $\simeq$ 0.01 % and the modal dampings with a precision of $\simeq$ 1 %. Moreover, this method allows for the identification of modal parameters of modes having a modal overlap up to 70 %.

5 Optimisation procedure

5.1 Estimation method

This section describes how to derive $\{E_x^H, \eta_x^H, E_y^H, \eta_y^H, G_{xy}^H, \eta_{xy}^H, G_{xz}^H, \eta_{xz}^H, G_{yz}^H, \eta_{yz}^H, \nu^H, \eta_\nu^H\}$ from the experimental values of the modal frequencies f_n^{XP} and dampings α_n^{XP}. Since the modal frequencies of the conservative and the real systems are equal to first order (section 3.1), it is valid to find separately and successively the elastic constants and the loss factors.

To first order, the modal frequencies depend only on the elastic constants of the homogeneous equivalent thick-plate model $\{E_x^H, E_y^H, G_{xy}^H, G_{xz}^H, G_{yz}^H, \nu^H\}$. Since this dependence is non-linear, a cost function C_E is defined (Eq. (21)) and an optimisation procedure based on the gradient-method has been implemented.

$$C_E = \sum_{n=1}^{N} \left(\frac{f_n^{XP} - f_n^{Num}}{f_n^{XP}} \right)^2 \tag{21}$$

It has been shown in section 3.3 that the damping coefficients $\{\alpha_n^{Num}\}_{n\in[1,N]}$ can be expressed as linear combinations of the $\{\eta_x^H, \eta_y^H, \eta_{xy}^H, \eta_{xz}^H, \eta_{yz}^H, \eta_\nu^H\}$ loss factors. Therefore, the latter can be obtained by a simple least mean square method, with the constraint that loss factors remain positive.

5.2 Results for the honeycombs core sandwich panel

5.2.1 Identification of elastic and damping constants

The optimisation is performed on the 45 first modal frequencies and dampings obtained experimentally for this panel. The numerical model used a $Q = 14$-order basis which proved to ensure the convergence of the highest modes values. The identified visco-elastic parameters of the equivalent homogeneous plate are given in Tab. 2. The relative errors in modal frequencies and dampings are shown in Fig. 2. It can be seen that the agreement is very good for modal frequencies (mean absolute error of 1.8 %). The predicted modal dampings fit well the mean measured ones, but the difference is more important (mean absolute error of 10.2 %).

	$\underline{E}_x^H$	$\underline{E}_y^H$	$\underline{G}_{xy}^H$	$\underline{G}_{xz}^H$	$\underline{G}_{yz}^H$	$\underline{\nu}_{xy}^H$	$\underline{\nu}_{yx}^H$
Real part	1.0 GPa	1.4 GPa	0.46 GPa	12 MPa	26 MPa	0.23	0.33
Loss factor (%)	1.3	1.4	1.1	4.4	8.1	0	0.1

Table 2: Identified parameters of the homogenised model corresponding to the honeycombs core sandwich panel. The coefficients in the two last columns are mutually related by the symmetry relationships (cf. section 2.2).

5.2.2 Sensitivity analysis

The sensitivities of the frequency values f_n to the coefficients $\{E_x^H, E_y^H, G_{xy}^H, G_{xz}^H, G_{yz}^H\}$ are defined as $S_{f_n}(X) = \frac{\partial f_n}{\partial X}\left(\frac{f_n}{X}\right)^{-1}$. They reflect the information contained in a modal frequency relatively to the elastic parameter X. Results are presented in Fig. 3. Since the modal frequencies are very little sensitive to the Poisson coefficients compared to the other in-plane parameters, their sensitivities to these parameters have not been represented. As expected, it can be seen in Fig. 3a that modes of the form $(0, i)$ or $(j, 0)$ convey a lot of information relatively to E_x and E_y respectively. Since the thick-plate model differs from the thin-plate model for the higher frequencies, it is normal that there is almost 10 times more information relative to G_{xz} and to G_{yz} in the higher modes than in the lower ones (Fig. 3b). The lower sensitivity of G_{xz} to the modal frequencies than that of G_{yz} is simply due to the aspect ratio of the plate ($l_x < l_y$).

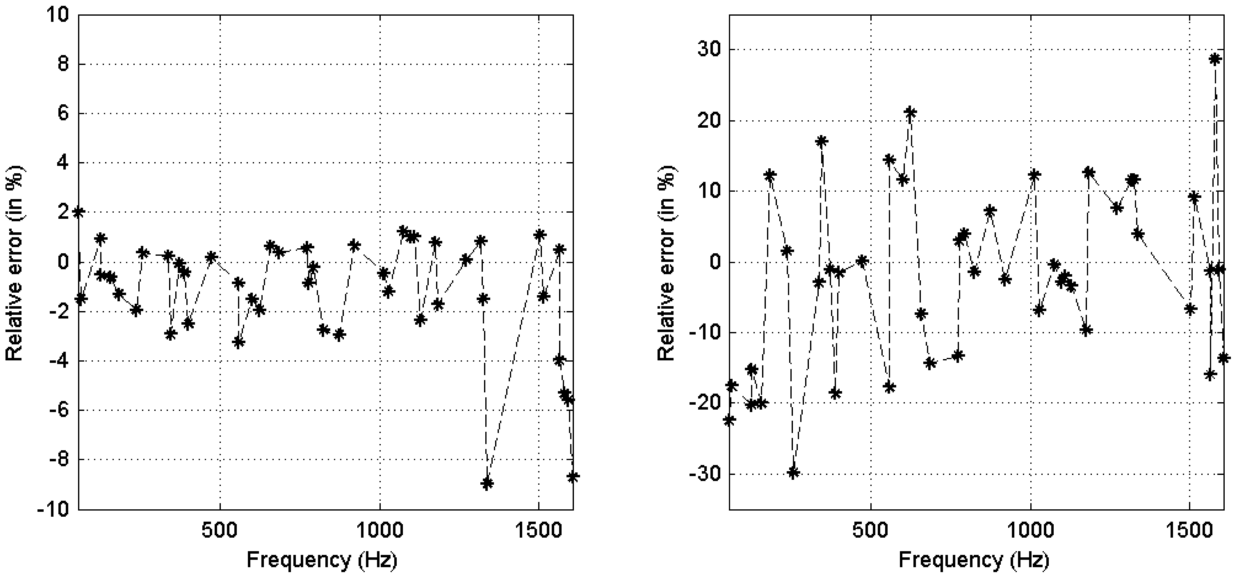

Figure 2: Comparisons between measured and predicted modal frequencies (left) and dampings (right) for the honeycomb sandwich panel.

5.3 Results for the corrugated core sandwich panel

5.3.1 Identification of elastic and damping constants

The optimisation is performed on the 38 first modal frequencies and dampings obtained experimentally for this panel. The numerical model used a $Q = 13$-order basis which proved to ensure the convergence of the highest modes values. The identified visco-elastic parameters of the equivalent homogeneous plate are given in Tab. 3. The relative errors in modal frequencies and dampings are shown in Fig. 4. It can be seen that the agreement is satisfying for modal frequencies (mean absolute error of 2.2 %). The predicted modal dampings fit correctly the mean measured ones, but as previously the difference is more important (mean absolute error of 36 %).

	$\underline{E}_x^H$	$\underline{E}_y^H$	$\underline{G}_{xy}^H$	$\underline{G}_{xz}^H$	$\underline{G}_{yz}^H$	$\underline{\nu}_{xy}^H$	$\underline{\nu}_{yx}^H$
Real part	116 GPa	102 GPa	46 GPa	78 GPa	163 GPa	0.32	0.28
Loss factor (%)	0.12	0.15	0.1	0	0	0.1	0.13

Table 3: Identified parameters of the homogenised model for the other sandwich panel. The coefficients in the two last columns are mutually related by the symmetry relationships (cf. section 2.2).

In Fig. 4, it can be seen that the error on damping estimation is moderate in the mid-frequency range, but larger for the first modes and in the high-frequency range. As the identified loss factors are very low (see Tab. 3), the measured modal dampings are very sensitive to the way the panel is suspended and to the damping due to acoustical radiation. In the present case, the thin wires used to suspend the panel may be the origin of some additional damping in the low frequency range that was not included in the model. In the high-frequency range, the damping is systematically underestimated above 3 kHz. Since the equivalent elastic parameters of the panel have been identified, the coincidence frequency of this panel can be estimated around 4 kHz. This results in an additional damping due to acoustical radiation as the modal frequency comes closer to this frequency. In the same spirit, the modal frequencies seem systematically underestimated by 2 % below 3 kHz. In order of magnitude, this is consistent with air loading in the low frequency range.

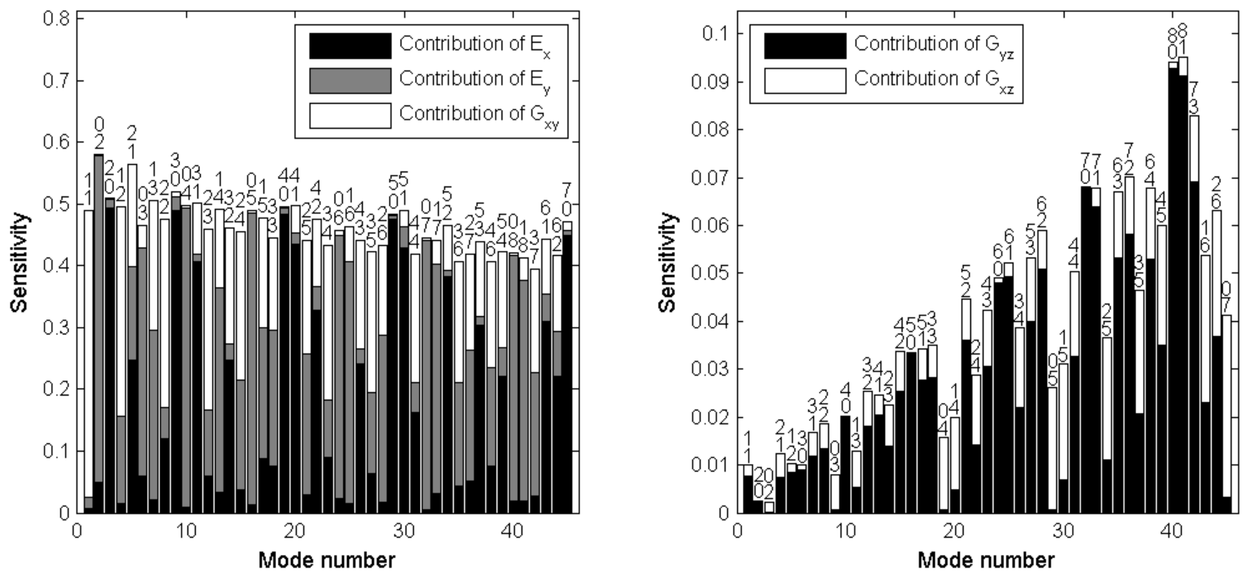

Figure 3: Sensitivities of the mechanical parameters to the modal frequencies for the honeycombs core sandwich panel. In the figures, each column is the sum of the sensitivities of the different involved parameters. On the top of the column the number of nodal lines in the x (top) and y (bottom) directions of this mode is specified .

5.3.2 Sensitivity analysis

Results of the sensitivity analysis are presented in Fig. 5. Since the modal frequencies are almost insensitive to the Poisson coefficients, their sensitivities to these parameters have not been represented. For this panel it can be seen that the sensitivity to the out-of-plane properties is very low compared to the sensitivity relative to the in-plane properties. This means that the modal frequencies and modal dampings are very little influenced by the out-of-plane complex moduli. As a consequence the estimations of these parameters are to be interpreted very carefully. In this case, even if the plate fulfills the hypothesis of the Reissner-Mindlin model (*i.e.* $l_{x,y}/h \simeq 90$), the core material has too high out-of-plane shear moduli to allow for their precise identification.

6 Conclusion

An identification method that yields all the mechanical parameters of sandwich materials that matter dynamically, under only mild hypotheses has been presented. The performances of the method have been illustrated successfully on two different sandwich panels having heterogeneous cores: paper honeycombs core and steel corrugated core.

Compared to the methods proposed in Refs. [7, 8], this method also provides loss factors. Compared to the methods presented in Refs. [4, 5, 6], out-of-plane complex moduli of the materials are also extracted. Compared to the method proposed in Ref. [1, 2, 3], this method is considerably easier and faster to implement since only one vibrating point is to be measured. It also reaches frequency domains that are usually out of reach of the modal analyses based on the Fourier transform. Incidentally, the method presented here could be used to access the frequency-dependence of the loss factors by considering only modes in a given frequency range. Compared to the static investigations on each sandwich component, this dynamical method is non-destructive and the experimental test needs very little time. Avoiding heavy lab-equipment, it is a good candidate for industrial in-line process of quality control.

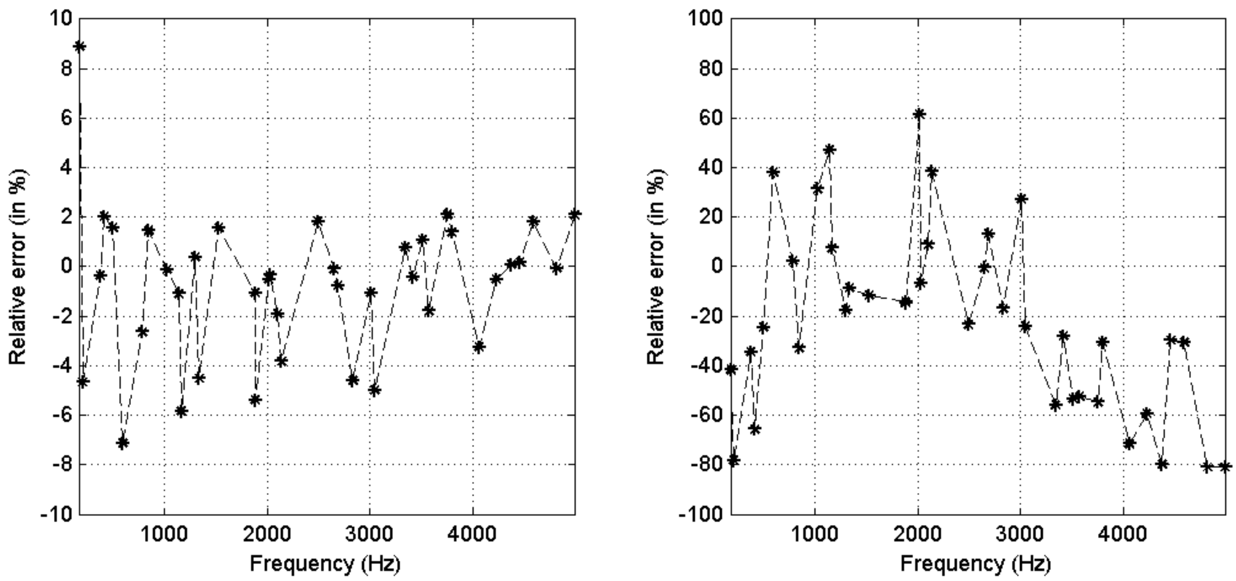

Figure 4: Comparisons between measured and predicted modal frequencies (left) and dampings (right) for the corrugated core panel.

Acknowledgements

Authors would like to thank Étienne Corteel, Camille Besse and Dirk Mohr for providing the different test samples that have been characterized in this paper.

References

[1] E. Pagnacco, A. Moreau, and D. Lemosse. Inverse strategies for the identification of elastic and viscoelastic material parameters using full-field measurements. *Materials Science and Engineering A-structural Materials Properties Microstructure and Processing*, 452:737–745, April 2007.

[2] M. Matter, T. Gmur, J. Cugnoni, and A. Schorderet. Numerical-experimental identification of the elastic and damping properties in composite plates. *Composite Structures*, 90(2):180–187, 2009.

[3] A. Giraudeau, F. Pierron, and B. Q. Guo. An alternative to modal analysis for material stiffness and damping identification from vibrating plates. *Journal of Sound and Vibration*, 329(10):1653–1672, May 2010.

[4] J. DeVisscher, H. Sol, W. P. DeWilde, and J. Vantomme. Identification of the damping properties of orthotropic composite materials using a mixed numerical experimental method. *Applied Composite Materials*, 4(1):13–33, 1997.

[5] J. P. Talbot and J. Woodhouse. The vibration damping of laminated plates. *Composites Part A-applied Science and Manufacturing*, 28(12):1007–1012, 1997.

[6] M. E. McIntyre and J. Woodhouse. On measuring the elastic and damping constants of orthotropic sheet materials. *Acta Metallurgica*, 36(6):1397–1416, 1988.

[7] S. F. Bastos, L. Borges, and F. A. Rochinha. Numerical and experimental approach for identifying elastic parameters in sandwich plates. *Shock and Vibration*, 9(4-5):193–201, 2002.

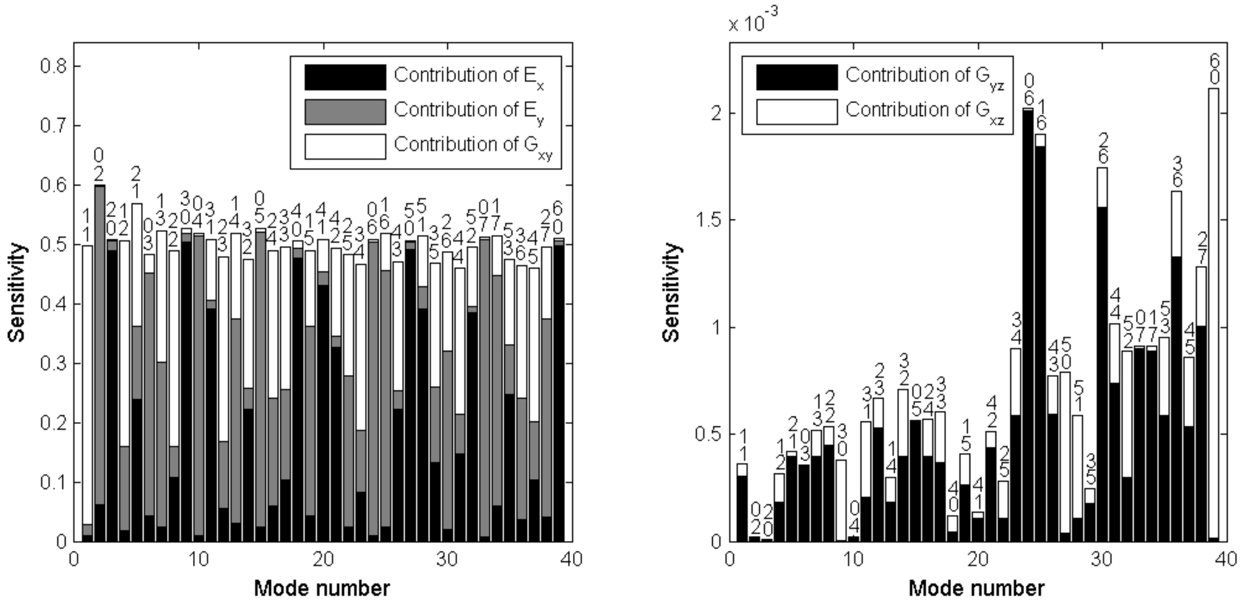

Figure 5: Sensitivities of the mechanical parameters to the modal frequencies for the corrugated core sandwich panel. In the figures, each column is the sum of the sensitivities of the different involved parameters. On the top of the column the number of nodal lines in the x (top) and y (bottom) directions of this mode is specified .

[8] M. N. Ichchou, O. Bareille, and J. Berthaut. Identification of effective sandwich structural properties via an inverse wave approach. *Engineering Structures*, 30(10):2591–2604, 2008.

[9] W. S. Burton and A. K. Noor. Assessment of continuum models for sandwich panel honeycomb cores. *Computer Methods in Applied Mechanics and Engineering*, 145(3-4):341–360, 1997.

[10] L. Cremer, M. Heckl, and B.A.T. Peterson. *Structure-Borne Sound: Structural Vibrations and Sound Radiation at Audio Frequencies Third Edition*. Springer-Verlag, 2005.

[11] K. Ege, X. Boutillon, and B. David. High-resolution modal analysis. *Journal of Sound and Vibration*, 325(4-5):852–869, 2009.

[12] M. Soula, R. Nasri, A. Ghazel, and Y. Chevalier. The effects of kinematic model approximations on natural frequencies and modal damping of laminated composite plates. *Journal of Sound and Vibration*, 297(1-2):315–328, October 2006.

[13] G. B. Muravskii. On frequency independent damping. *Journal of Sound and Vibration*, 274(3-5):653–668, July 2004.

[14] E. Nilsson and A. C. Nilsson. Prediction and measurement of some dynamic properties of sandwich structures with honeycomb and foam cores. *Journal Of Sound And Vibration*, 251(3):409–430, March 2002.

[15] E. O. Ayorinde. Elastic constants of thick orthotropic composite plates (vol 29, pg 1025, 1995). *Journal of Composite Materials*, 30(15):1729–1729, 1996.

[16] V. Birman. On the choice of shear correction factor in sandwich structures. *Journal of Sandwich Structures & Materials*, 4(1):83–95, 2002.

[17] M. Geradin and D. Rixen. *Mechanical Vibrations: Theory and Applications to Structural Dynamics*. 1997.

[18] R. B. Bhat. Natural frequencies of rectangular-plates using characteristic orthogonal polynomials in Rayleigh-Ritz method. *Journal of Sound and Vibration*, 102(4):493–499, 1985.

[19] M. Rébillat, R. Hennequin, E. Corteel, and B. F. G. Katz. Prediction of harmonic distortion generated by electro-dynamic loudspeakers using cascade of Hammerstein models. *128th Convention of the Audio Engineering Society*, 2010.